Scattering mechanism of electrons interacting with surfaces in specular reflection geometry: Graphite

A. Ruocco and M. Milani
Dipartimento di Fisica, Università Roma Tre and Unità INFM Roma Tre, Via della Vasca Navale 84, I-00146 Roma, Italy

S. Nannarone
Dipartimento di Fisica, Università di Modena and Unità INFM Modena, Via Campi 213a, 41100 Modena, Italy

G. Stefani
Dipartimento di Fisica, Università Roma Tre and Unità INFM Roma Tre, Via della Vasca Navale 84, I-00146 Roma, Italy
(Received 15 September 1998)

We have studied the scattering mechanism of electron-energy-loss process in specular reflection geometry highlighting the presence of an elastic collision that always accompanies the inelastic one. It implies that two independent channels contribute to the inelastic cross section depending on whether the inelastic event precedes or follows the elastic one. Our results indicate that neither one of the channels is favored by propensity rules. Nevertheless, suitable experimental conditions permit to enhance contribution to the cross section of one channel with respect to the other. The possibility to single out the contribution of a given channel allows to determine without ambiguity the momentum exchanged in the inelastic collision. This is of fundamental relevance for several electron impact spectroscopies, such as electron-energy-loss spectroscopy and *(e,2e)*, in specular reflection geometry. These results are derived from measuring the current of elastically and inelastically specularly reflected electrons as a function of the primary electron beam kinetic energy (IV curve). The incident beam energy was varied between 150 and 450 eV, the target was an highly oriented pyrolitic graphite and the range of losses investigated was 6–35 eV. A simple kinematics model that accounts for refractive effects due to the surface potential barrier, gives good agreement with the observed diffraction pattern of the elastically reflected electrons. [S0163-1829(99)01519-2]

I. INTRODUCTION

The elastic and inelastic scattering of electron has been widely used to study the properties of matter. In particular the specular reflection geometry has been used to study the surface properties of solids. In this particular geometry, due to the short mean-free path in the matter, the penetration depth is reduced to the first few layers thus, enhancing the surface signal for both elastic and inelastic events.

In this paper, we deal with the fundamental question of which is the dominant mechanism for inelastic scattering of electron in specular reflection geometry. The question of whether the inelastically scattered electron is originated by a single inelastic event or by a sequence of elastic and inelastic events is still partially unanswered. To answer it is of fundamental relevance in order to correctly interpret the results of the various electron-energy loss (EEL) spectroscopies in reflection geometry. In fact, the concomitant presence of the elastic event changes drastically the momentum exchanged in the inelastic one. In the single-scattering model the inelastic event accounts for the large momentum exchanged, which is necessary to reflect the electron from the surface. In the double scattering model, the reflection originates from the elastic interaction with the solids and the inelastic event is essentially in forward direction and it is associate to a small momentum transfer. It is only in the latter case that the dipole approximation can be applied to calculate inelastic cross section.[1] The knowledge of the electron scattering mechanism on surfaces is also necessary to the interpretation of *(e,2e)* experiments.[2] This spectroscopy rely on an unambiguous momentum balance in order to reconstruct the target valence band[3] and the associate momentum density.[4]

More precisely, the paper is aimed at discerning under which experimental conditions the double collision model will be more appropriate than the single collision one to describe electron scattering spectroscopies from surfaces.

From the theoretical point of view the problem has been widely dealt with by several authors. Among others we remember the work of Mills and coworkers[5] on the interaction of electron with collective excitations of solids. They come to the conclusion that in specular reflection geometry the inelastic event is followed or preceded by an elastic event. This conclusion is valid in a wide range of energy loss, from meV to tenth of eV. Analogous conclusion are reached by Saldin[6] in his work on the ionization of the inner shell (1S) of carbon where the energy loss is about 290 eV; in this case the transition involved is not any more collective but a single-particle one. These works then suggest that in reflection geometry the inelastic event is always assisted by an elastic collision and this is true in a wide range of energy loss independently of the particular type of excitation. As a consequence two channels contribute to the energy-loss cross section: elastic before loss $(D+L)$and elastic after loss $(L+D)$. Saldin[6] foresees that the two channels should have amplitudes of comparable magnitude and that interference effects are possible.

From the experimental point of view the double mechanism associated with the reflection EEL process is widely

accepted and used to analyze the experimental data but a clear evidence for validity of this model is still missing. A search for such an evidence was first attempted in the thirties and the presence of a double mechanism pointed out, but the primitive experimental conditions did not allow to clearly disentangle contributions of the two channels ($L+D$ or $D+L$) of scattering.[7]

More recently, different authors[8–10] have successfully employed the double scattering mechanism to analyze their experimental data of reflection EEL spectroscopy, thus giving an indirect confirmation of the validity of this mechanism. The problem of highlighting double collision process has been recently dealt with by Gunnella *et al.*[11] that studied the relative probability of the two channels, $D+L$ and $L+D$, in core excitation of graphite. They studied the angular behavior of reflection EEL features appearing in the region of carbon *K* edge in highly oriented pyrolitic graphite (HOPG) at a fixed incident energy of 500 eV. The energy loss of the involved transitions are 285 eV ($1s\rightarrow\pi^*$) and 292 eV ($1s\rightarrow\sigma^*$). In their experimental condition, the $L+D$ channel dominates the cross section. To reach this conclusion it was necessary to compare experimental data with theory.

The present paper achieves two main goals: (i) to experimentally demonstrate that in the reflection energy-loss scattering the double collision model is correct; (ii) to investigate the relative probability of the two channels, $L+D$ and $D+L$.

The intensity of elastic and inelastic electron current specularly reflected from HOPG has been measured as a function of the incoming electron energy at fixed geometry (IV curve). In the low-energy electron diffraction (LEED) technique the analysis of IV curve of elastically scattered electron is a standard procedure to get structural information of the target.[12] In particular, the specular reflection geometry has been already used to study the mean interatomic distance in amorphous materials[13] by measuring elastic IV and to give structure information in terms of surface holograms[14] by measuring inelastic IV.

In order to analyze the elastic IV curve refraction of electron at the surface (originated by the inner potential) must be taken into account.[15] We have used a kinematic model to interpret the IV data with inner potential as a fitting parameter. As a consequence, whenever the target geometry is known, this method provides an independent determination on the inner potential value.

The paper is organized in five sections: the experimental apparatus and some information on the sample preparation are presented in the following section; in Sec. III are presented and discussed the data regarding the elastic scattering and the inner potential determination; in the fourth section are presented and discussed the data on the inelastic scattering while conclusions are drawn in the last section.

II. EXPERIMENT

The experiment was performed at the Department of Physics of the Università di Roma Tre with a new apparatus originally developed for electron and ion spectroscopies. It mainly consists of an electron gun, a sample manipulator and two electron analyzers. The electron gun optics is a commercial one by Varian powered by programmable power supplies in order to perform automatic scan of the electron energy in the range 50–600 eV. Voltages of the focusing element and deflector plates are driven by the same analog signal that sets the beam energy. This is done in order to achieve constant size and position for the beam spot during the energy scans. The manipulator is a commercial VG model HPT-WX while the electron analyzers have been developed in our group: they consist of an hemispherical dispersive element plus a system of electrostatic lenses. Only one of the two electron analyzers is used for this experiment. The principal features of this analyzer are: angular resolution of 1.5° full width at half maximum (FWHM) and energy resolution of 400 meV at 20 eV of pass energy. For what concerns the absolute value of the incident energy we estimate a reproducibility of ± 500 meV and a precision of ± 1 eV.

The analyzer is polarized by programmable power supplies and a single acquisition program permits control at the same time the electron gun energy and the analyzed energy. By controlling these two parameters the probability of the energy loss is measured as a function of the primary energy and of the scattered electron energy.

To avoid radiation damage of the surface a low current was used: typically 25 pA at 200 eV for the elastic IV curves and 350 pA at 200 eV for the inelastic IV curves. The incident current on the sample is monitored during the experiment to take into account the variation of the electron flux with the kinetic energy. The whole set of spectra was collected in the pulse counting mode.

The IV raw data were normalized to the incident current and for the transmission of the electron analyzer. The latter normalization takes into account that the analyzer was set at fixed pass energy (20 eV) and consequently the transmission changes as a function of the retarding factor (i.e., the ratio between the analyzed energy and the pass energy). Nevertheless, to measure the relative amplitude of maxima in the IV elastic curve was not one of the main thrust of this work and it was not verified that this quantity is purged by all possible systematic errors.

The HOPG samples were peeled in air with Scotch tape and quickly inserted in the vacuum chamber where it was then annealed at 600 °C; the base pressure, in the vacuum vessel was 4×10^{-10} torr.

Surface order and cleanness were monitored measuring the width of the elastic peak angular distribution around the specular reflection. Typical FWHM was 1.5 degrees. Using low-incident electron current the width of angular distribution does not change after several days of measurements.

The quality of the surface was also monitored comparing the EEL spectrum taken just after the annealing to those taken at later times. In particular, the relative intensity of the loss peak at 6 eV, assigned to a transition which involve surface states, is known to be very sensitive to the cleanness and order of the surface.[16]

III. ELASTIC SCATTERING: PRESENTATION AND DISCUSSION

In Fig. 1 is reported the intensity of the elastic electron current specularly reflected from HOPG surface as a function of the kinetic energy of the incident electron (IV curve). The

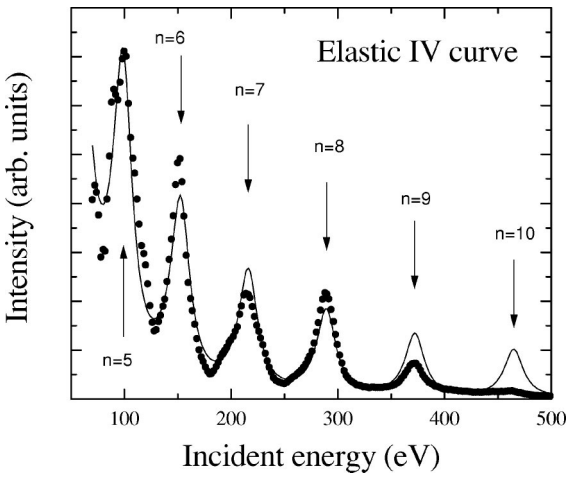

FIG. 1. The black dots represent the intensity of elastic electron specularly reflected from HOPG surface as a function of the kinetic energy of incident electron. The arrows indicate the position of diffraction peak maxima calculated with expression (1) and with $V_o = 16$ eV. Behind each arrow is indicated the value of the diffraction order n. The continuous line is the result of the calculation explained in the text.

incidence angle of the electron beam was $\Theta = 34°$. Each point of the spectrum represents the intensity of the current of reflected electrons as derived from a Gaussian fit of the elastic peak measured scanning the analyzed energy. In this spectrum there are three features that must be highlighted: first of all the strong modulation in the intensity that can be ascribed to the Bragg interference between electron reflected from successive planes along C axis of graphite.[12] The second feature is the decay of the intensity of the peaks as a function of the increasing energy. Last observation is on the profile of the diffraction peaks: in the case of the peaks labeled $n = 7,8$ it is evident the presence of a shoulder at lower kinetic energy that evolves in a doublet for $n = 5$.

In the case of the HOPG, the periodicity in the plane perpendicular to the C axis is lost and the one existing is along the C axis is the origin for the observed diffraction effects.

To explain the position of the maxima in the curve of Fig. 1, the Bragg diffraction theory is adequate within the space of the solid. In fact incoming electrons are strongly refracted from the barrier potential encountered at the surface: their direction inside the solid is different from the one they had outside.[15] The positions of the maxima is well accounted if refractive and diffraction effects are considered at the same time; under these conditions, the Bragg law can be written as:

$$E_{\max} = \left(\frac{\hbar^2 \pi^2}{2 m_e d^2} n^2 - V_o \right) \frac{1}{\cos^2 \theta}, \tag{1}$$

where V_o is the real part of the inner potential, n is the order of the Bragg diffraction, θ is the incidence angle of the incoming electron and d is the spacing between planes: in this case $d = 3.35$ Å;[17] half the periodicity along the C axis. Expression (1) can be used to estimate the value of the inner potential V_o. In fact, the position of the maxima can be fitted with Eq. (1) using V_o as a free parameter. The best overall fit, of the measured maxima in the *IV* curve, is obtained with $V_o = 16 \pm 1$ eV. This value is in good agreement with those reported in literature.[18] In Fig. 1 the arrows represent the position of maxima calculated with expression (1) and with $V_o = 16$ eV.

In Fig. 1, the continuous line represents the result of the IV predicted by a kinematics model that takes into account refraction and absorption of incident electron at the surface. In this model the first Born approximation was applied, consequently the cross section is the product of two terms: the structure factor and the atomic form factor, both depending on the exchanged momentum transfer. The first term determines the oscillation (diffraction). The atomic form factor is calculated using a screened Coulomb potential and determines the attenuation of the intensity as a function of the primary energy. The wave function of the electron inside the sample is modified by the complex inner potential that takes into account the interaction of the primary beam with the conduction- and valence-band electron. In particular, the real part of the inner potential influences the position maxima while the imaginary part determines the shape of the peaks. The continuous curve in Fig. 1 has been calculated using the real and imaginary part of the inner potential as free parameters and fitting them to the experimental data. The best fit was obtained with 15.6 ± 1 eV for the real part and 7.5 ± 1 eV for the imaginary part of the inner potential. The values of the real part of the inner potential obtained with the two methods are equal within the error bars.

Two noticeable discrepancies are found between experiment and theory. At low energy, the experimental peak shape is more complex than the theoretical one. The purely kinematic approach adopted is not adequate to account for multiple scattering events that became relevant at low-incident energies. These dynamic effects show up in the IV curve with a further peak near peak $n = 5$ and with a shoulder in peaks $n = 7$ and $n = 8$. At high energy the calculated shape agrees well with the experiment while the relative intensity of the peaks in not well accounted. As already discussed in the experimental section to accurately measure relative intensity was not the aim of this paper.

IV. INELASTIC SCATTERING: PRESENTATION AND DISCUSSION

In Fig. 2 are reported the IV spectra taken at different loss energies as a function of the kinetic energy of incoming electron. Each spectrum is measured at a fixed energy loss ΔE_{Loss} scanning the incoming electron energy E_i and setting the analyzed energy E_A according to the following relation

$$E_A = E_i - \Delta E_{Loss} \tag{2}$$

consequently, each excitation spectrum represents the probability of loss ΔE_{Loss} as a function of the incident energy. In the figure is also reported the spectrum at $\Delta E_{Loss} = 0$ eV, that is the spectrum of elastically reflected electron.

The energy losses selected for measuring the excitation spectra are visualized by arrows in Fig. 3 where they are

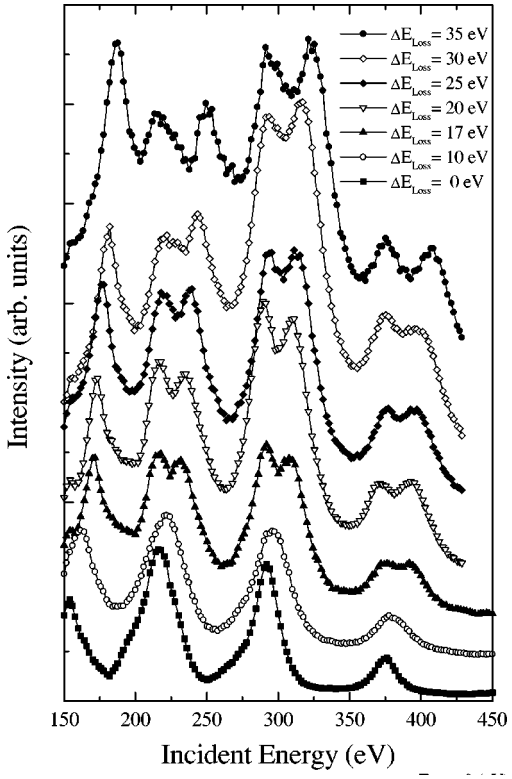

FIG. 2. Excitation spectra taken at different energy loss. Each spectrum is taken at fixed energy loss as a function of the energy of incident electron. For each point the analyzed energy is set according to the expression (2).

reported alongside a typical HOPG EEL spectrum as measured with an incident energy of 203 eV.

From Fig. 2 it is evident that there is a continuous evolution of the excitation spectra as the energy loss increases. In the spectrum at $\Delta E_{Loss}=10$ eV each peak of the elastic spectrum ($\Delta E_{Loss}=0$ eV) is present with an increased width. In

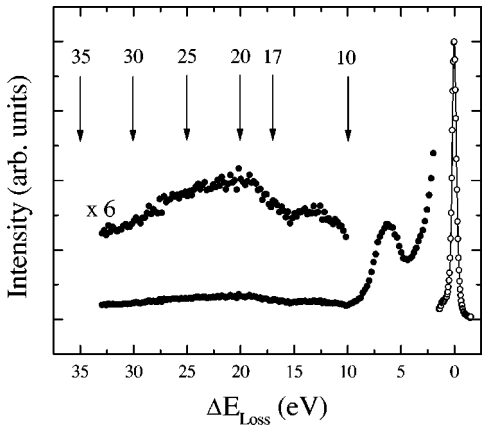

FIG. 3. Typical reflection EEL spectrum taken at 203 eV of incident electron energy and incident angle of 34°. The loss region (●) is taken with an incident current of 350 pA while the elastic region (○) is taken with an incident current of 25 pA. Part of the loss region is enhanced to point out the presence of two structures whose maxima are at 13 and 20 eV. The arrows indicate the energy loss selected for measuring the excitation spectra reported in Fig. 2.

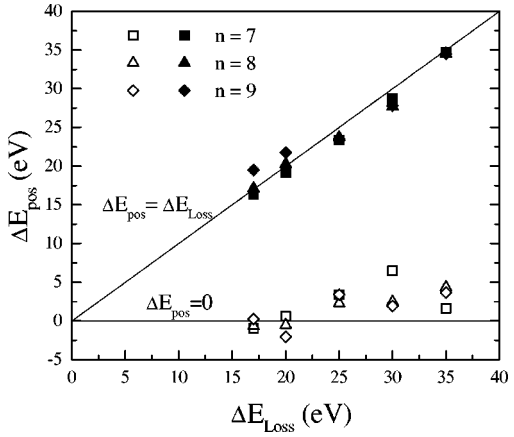

FIG. 4. Energy position of the maxima in the excitation spectra of Fig. 3 as a function of the selected energy loss. Each point of this figure corresponds to a maximum in the excitation spectra of Fig. 3. In particular are reported the positions of the 6 maxima present in each spectrum of fixed energy loss (ΔE_{Loss}): 3 for the main peaks (open symbol, $n=6,7,8$) and 3 for the associated replica peaks (solid symbol). The peak positions (ΔE_{pos}) are measured with respect to the corresponding peaks in the elastic IV curve of Fig. 1.

the successive spectra ($\Delta E_{Loss}>10$ eV) the peaks present in the elastic spectrum split in two components: the first peak of the doublet remains at the same energy of the corresponding peak in the elastic spectrum while the second component shifts away as the energy loss ΔE_{Loss} increases. In the following discussion we will call main peaks those component of the inelastic spectrum that appear at the same energy of the elastic one; the new component of the inelastic spectrum will be called replica; finally, we define doublet a specific main peak together with his replica.

The two components of the doublet can be resolved only for $\Delta E>13$ eV and the splitting between main peak and replica is found to be almost identical to the energy loss value. This finding is clearly summarized in Fig. 4 where position (ΔE_{pos}) of the maxima of the main and replica peaks, relative to the corresponding elastic excitation peak, are reported. From this figure is evident that the main peak of each doublet remains substantially at the same energy position of the spectrum taken at loss $=0$ eV ($\Delta E_{pos}=0$) while the replica shifts at higher energy by a quantity equal to the corresponding loss: in fact the points corresponding to the position of the replica are aligned along the straight line of equation $\Delta E_{pos}=\Delta E_{Loss}$.

The major features appearing in Fig. 2 and Fig. 4 can be explained by the following model: the EELS in specular reflection geometry is the result of a double scattering mechanism: the incident electron undergoes two independent collision: elastic and inelastic. As already mentioned the elastic process can follow or precede the inelastic one giving rise to two independent channels: $L+D$ and $D+L$, respectively. In this framework the EEL cross section is the product of the elastic cross section times the inelastic one. Much of the modulation present in Fig. 2 is ascribable to the elastic component of the cross section because the forward inelastic component changes smoothly with the incoming energy.

To test the validity of this model it is sufficient to analyze one doublet. The main peak is originated by the $(D+L)$

channel. In this case the elastic reflection occurs with the same energy of the incident electron and as a consequence the modulation in the intensity of this process reproduces the modulation of the elastically reflected electron (see Fig. 1). The replica is originated from the channel $L+D$. In fact, in this case the elastic reflection occurs at an energy equal to the incident electron energy minus the energy lost in the scattering. Assuming that the modulation in the intensity of the spectra at fixed loss derive only from the modulation in the elastic scattering process, the process $(L+D)$ gives rise to the same modulation of the elastic excitation spectrum shifted in energy by a quantity equal to the selected loss. Correctness of this assumption is evident looking at the spectra in Fig. 4 where the position of the second component of each peak increases the shift from the first component exactly by the same amount of the selected loss. Some of the points in Fig. 4 deviate from the straight lines $\Delta E_{pos} = \Delta E_{Loss}$ and $\Delta E_{pos} = 0$ more than the estimated uncertainty of ± 1.4 eV. This deviation from the linearity has been consistently reproduced by several independent measurements. We ascribe this deviation to the simplicity of the analysis used to find the position of the maxima in the inelastic IV curve. In fact, apparent maxima are strongly influenced by the shape of the curve and by the closeness of neighboring peaks. For instance, the shoulder at lower energy of the peak $n=7$, $\Delta E_{Loss}=30$ eV influences the position of the apparent peak maximum by 3.5 eV.

The similarity of the excitation spectra appearing in Fig. 2 with the spectrum at loss $=0$ indicates that the model is valid irrespective of the kind of excitation selected.

A quantum theory of the interaction of electron with the matter should include at the same time both channels $(D+L$ and $L+D)$ thus taking into account possible interference between them. In the same way, the theory should consider as a single process the two steps of each channel. Although this is true in principle, our experimental results indicate that in practice the elastic and the inelastic scattering can be considered as separate processes and the channel $D+L$ and $L+D$ can be treated independently, at least in the case of HOPG in the experimental conditions investigated.

Another qualitative conclusion that can be derived from the experimental results is about the branching ratio between the two channels contributing to the loss process; observing the spectra in Fig. 2 it is possible to conclude that the two channels, $D+L$ and $L+D$, have roughly the same probability to occur. This result is different from the conclusion of the article by Gunnella *et al.*[11] where it was pointed out a predominance in the probability of the $L+D$ channel. These different findings are to be ascribed to the different kinematical conditions of the two experiments. In fact, in their case the energy loss (290 eV) was large with respect to the incident energy (500 eV), hence the energy at which the impinging electron undergoes the elastic scattering changes much: in the $L+D$ channel the elastic scattering happens at $E_i - \Delta E_{Loss}$, while in the $D+L$ channel it happens at the energy E_i. The difference in the energy at which the elastic scattering happens, determines the difference in the probability for the two channels $L+D$ and $D+L$; this is due to the atomic cross section that has a strong monotonic dependence with the energy.[19]

From Fig. 2 it is evident that in the EEL process there is no *a priori* preference for one of the two channels ($L+D$ and $D+L$). It is by means of the selection of the experimental condition (incident energy, angle of incidence, and selected loss) that the cross section of one channel became predominant with respect to the other. It is evident that when the incident energy coincide with a main peak the channel $D+L$ is favorite respect to the $L+D$ channel. On the contrary, the $L+D$ channel is predominant at the energy of the replica peak.

The capability of controlling the relative weight of one channel with respect to the other can be useful to remove the uncertainty in the momentum transfer in an angle-resolved EEL experiment. In fact to each scattering channel is associated a different momentum transfer and if both channels are present at the same time, the momentum transfer vector of the experiment is not defined.

V. CONCLUSIONS

We have demonstrated that in our experimental condition (incident electron 100–500 eV and small energy losses 0–35 eV) the inelastic scattering is always accompanied by the elastic scattering: in particular the latter can follow or precede the former scattering giving rise to two independent channels $L+D$and $D+L$. The total cross section of an EEL experiment is then accounted for by the incoherent sum of the two scattering channels $L+D$and $D+L$ and the interference between them is negligible. This is an experimental confirmation of the theoretical prediction of Saldin.[6]

From the energy position of the diffraction peak in the elastic spectrum we were able to obtain the inner potential of HOPG. In fact the correct position of the peak are reproduced only if we consider the effects of the refraction of the electrons at the surface. This technique can be usefully employed to determine the inner potential of the target if it is known its structure.

The presence of the elastic event associated to the inelastic one implies that in an EEL experiment in specular reflection geometry, the momentum transfer in the inelastic event is minimized. It is then possible to apply the dipole approximation to calculate the cross section of the EEL experiment.

In summary, the findings of this paper constitute a direct experimental evidence for validity of the double collision model commonly adopted in describing EELS and *(e,2e)* experiments performed under specular reflection geometry.

ACKNOWLEDGMENTS

We are grateful to EEC HCM Research Networks Contract No. CHRX-CT930350, to Progetto Coordinato CNR, Comitato Nazionale Scienze Fisiche, and to MURST ''Progetti di ricerca di rilevante interesse nazionale'' for partial financial support to this work. One of us (A.R.) is grateful to the Università di Modena for support.

[1] H. Luth, *Surfaces and Interfaces of Solids* (Springer Verlag, Berlin, 1993), Chap. 4.1.
[2] M. Vos and I. E. McCarthy, Rev. Mod. Phys. **67**, 713 (1995).
[3] A. S. Kheifets, S. Iacobucci, A. Ruocco, R. Camilloni, and G. Stefani, Phys. Rev. B **57**, 2545 (1998).
[4] S. Rioual, S. Iacobucci, D. Neri, A. S. Kheifets, and G. Stefani, Phys. Rev. B **57**, 7360 (1998).
[5] H. Ibach and D. L. Mills, *Electron Energy Loss Spectroscopy and Surface Vibrations* (Academic, New York, 1982).
[6] D. K. Saldin, Phys. Rev. Lett. **60**, 1197 (1988).
[7] J. C. Turnbull and H. E. Farnsworth, Phys. Rev. **54**, 509 (1938).
[8] N. R. Avery, Surf. Sci. **111**, 358 (1981).
[9] F. P. Netzer and M. M. El Golmati, Surf. Sci. **124**, 26 (1983).
[10] A. G. Nassiopoulos and J. Cazaux, Surf. Sci. **149**, 313 (1985).
[11] R. Gunnella, I. Davoli, R. Bernardini, and M. De Crescenzi, Phys. Rev. B **52**, 17 091 (1995).
[12] J. B. Pendry, *Low-Energy Electron Diffraction* (Academic, New York, 1974).
[13] A. B. Bondarchuk, S. N. Goysa, I. F. Koval, P. V. Mel'nik, and N. G. Nakhodkin, Surf. Sci. **258**, 239 (1991).
[14] L. S. Caputi, O. Comite, A. Amoddeo, G. Chiarello, S. Scalese, E. Colavita, and L. Papagno, Phys. Rev. Lett. **77**, 1059 (1996).
[15] H. Luth, *Surfaces and Interfaces of Solids* (Springer Verlag, Berlin, 1993).
[16] S. Iacobucci, P. Letardi, M. Montagnoli, P. Nataletti, and G. Stefani, J. Electron Spectrosc. Relat. Phenom. **67**, 479 (1994).
[17] A. Hoffman, G. L. Nyberg, and J. Liesegang, Phys. Rev. B **45**, 5679 (1992).
[18] A. Hoffman, G. L. Nyberg, and S. Prawer, J. Phys.: Condens. Matter **2**, 8099 (1990).
[19] B. H. Bransden and C. J. Joachain, *Physic of Atoms and Molecules* (Longman, London, 1983).